Torque Ripple Reduction Method of Permanent Magnet Synchronous Motor by Current Sensor Gain Unbalance Correction

Jun-ichi Itoh, Yuuki Ikarashi, Koroku Nishizawa and Hiroshi Tamura
Department of Electrical Engineering
Nagaoka University of Technology
Nagaoka, Niigata, Japan
itoh@vos.nagaokaut.ac.jp

***Abstract*— This paper presents a new algorithm, which corrects gain unbalances of current sensors, applied in a conventional two-phase current detection for adjustable speed drive system of IPMSM. The gain unbalance of current sensors is corrected by utilizing the second harmonic components which is extracted by Discrete Fourier Transform (hereafter DFT) from q-axis voltage command. Besides, the correction process is performed in synchronization with the process of DFT. The validity of the proposed method is confirmed by experimental results. The torque ripples of the second harmonic components caused by the gain unbalance of current sensors is reduced by 94%.**

I. INTRODUCTION

Recently, motor drive systems using power electronics technologies which realize saving energy are rapidly becoming widespread due to increasing global environmental regulations. Particularly, a permanent magnet synchronous motor (hereafter PMSM) has a high efficiency and a small size compared with an induction motor. Thus, the PMSM is applied to the driving source of electric vehicle [1-3]. In order to further improve the efficiency and a torque control performance of the motor drive systems using the PMSMs, it is important to reduce torque ripple. The torque ripple is caused by spatial harmonics of a permanent magnet flux of the PMSM, the dead time of a voltage source inverter, and current sensor detection errors. Especially, the current detection is important to improve the performance. The current sensor detection errors can be generally classified into two categories, an offset error and a gain error.

Many on-line compensation methods for the current sensor detection errors have been researched [4-6]. Ref. [4] utilized an integral output of the d-axis current to compensate for the current sensor detection errors. However, the compensation performance heavily depends on an accuracy of a feed-forward back EMF in the current controller. Ref. [5, 6] utilizes the voltage command generated by a current controller to compensate for the current sensor detection errors. However, these compensation performances deteriorate with increasing the motor parameter errors. These compensation methods require the motor parameters, such as a winding inductance or a back EMF, for reducing the torque ripples. Then, another algorithm that can compensate for the current sensor detection errors without using the motor parameters has been also reported by authors [7-9]. These method can compensate the current sensor offset errors by using DC voltage components included in phase voltage commands. However, these compensation method cannot correct the gain unbalance of the current sensors.

This paper presents a new correction method for the gain unbalance of the current sensors at a two-phase current detection system for driving Interior PMSM (hereafter IPMSM) without using the motor parameters. Firstly, the proposed correction method extract the second harmonic components, which is caused by the unbalance of the current sensors gain and included in the q-axis voltage command generated by the current controller, by DFT. Then, by compensating V-phase gain so as to match U-phase gain, the gain unbalance of the current sensors is corrected.

In this paper, Section II describes the proposed algorithms for correcting the gain unbalance of the current sensors. Section III discusses the effectiveness of the proposed method with reference to experimental results.

II. PROPOSED CORRECTION METHOD OF GAIN UNBALANCE

A. *Torque ripples resulting from the detection errors of the current sensors*

Fig. 1 shows the conventional adjustable speed drive system of IPMSM with two-phase current detection.

Detected dq-axis currents i_d^{cs} and i_q^{cs} are calculated from the phase currents i_u^{cs} and i_v^{cs} which are detected at the U and V-phase current sensors.

$$\begin{bmatrix} i_d^{cs} \\ i_q^{cs} \end{bmatrix} = \frac{2}{3}\begin{bmatrix} \cos\theta & \cos\left(\theta-\frac{2}{3}\pi\right) & \cos\left(\theta+\frac{2}{3}\pi\right) \\ -\sin\theta & -\sin\left(\theta-\frac{2}{3}\pi\right) & -\sin\left(\theta+\frac{2}{3}\pi\right) \end{bmatrix}\begin{bmatrix} i_u^{cs} \\ i_v^{cs} \\ -i_u^{cs}-i_v^{cs} \end{bmatrix} \quad (1)$$

where θ is a motor's electrical angle.

Equation (1) can be expressed as (3) by defining the detected dq-axis currents as (2).

$$\begin{cases} i_u^{cs} \approx G_u^{cs} I_m^{true} \cos(\theta+\phi) + I_{uoffset}^{cs} \\ i_v^{cs} \approx G_v^{cs} I_m^{true} \cos\left(\theta-\frac{2}{3}\pi+\phi\right) + I_{voffset}^{cs} \end{cases} \quad (2)$$

$$\begin{bmatrix} i_d^{cs} \\ i_q^{cs} \end{bmatrix} \approx \frac{2}{3}\begin{bmatrix} \cos\theta & \cos\left(\theta-\frac{2}{3}\pi\right) & \cos\left(\theta+\frac{2}{3}\pi\right) \\ -\sin\theta & -\sin\left(\theta-\frac{2}{3}\pi\right) & -\sin\left(\theta+\frac{2}{3}\pi\right) \end{bmatrix} \cdot \begin{bmatrix} G_u^{cs} I_m^{true} \cos(\theta+\phi) + I_{uoffset}^{cs} \\ G_v^{cs} I_m^{true} \cos\left(\theta-\frac{2}{3}\pi+\phi\right) + I_{voffset}^{cs} \\ -G_u^{cs} I_m^{true} \cos(\theta+\phi) - G_v^{cs} I_m^{true} \cos\left(\theta-\frac{2}{3}\pi+\phi\right) - I_{uoffset}^{cs} - I_{voffset}^{cs} \end{bmatrix} \quad (3)$$

where G_u^{cs} is a detection gain of U-phase current sensor, G_v^{cs} is a detection gain of V-phase current sensor, ϕ is a phase difference between a pole position θ and the detected motor current, $I_{uoffset}^{cs}$ is a detected offset current in current sensor of U-phase, $I_{voffset}^{cs}$ is a detected offset current in current sensor of V-phase, I_m^{true} is a true amplitude of fundamental current.

From (3), it is found that the detected dq-axis currents contain dc-components, fundamental frequency components and second harmonic components. These components can be separated by using addition theorem.

$$\begin{bmatrix} i_d^{cs} \\ i_q^{cs} \end{bmatrix} \approx \frac{I_m^{true}}{\sqrt{3}}\begin{bmatrix} G_u^{cs} \sin\left(\frac{2}{3}\pi+\phi\right) + G_v^{cs} \sin\left(\frac{2}{3}\pi-\phi\right) \\ -G_u^{cs} \cos\left(\frac{2}{3}\pi+\phi\right) + G_v^{cs} \cos\left(\frac{2}{3}\pi-\phi\right) \end{bmatrix}$$
$$-\frac{2}{\sqrt{3}}\begin{bmatrix} I_{uoffset}^{cs} \sin\left(\theta-\frac{2}{3}\pi\right) - I_{voffset}^{cs} \sin\theta \\ I_{uoffset}^{cs} \cos\left(\theta-\frac{2}{3}\pi\right) - I_{voffset}^{cs} \cos\theta \end{bmatrix}$$
$$-\frac{I_m^{true}}{\sqrt{3}}\begin{bmatrix} \left(G_u^{cs}-G_v^{cs}\right) \sin\left(2\theta-\frac{2}{3}\pi+\phi\right) \\ \left(G_u^{cs}-G_v^{cs}\right) \cos\left(2\theta-\frac{2}{3}\pi+\phi\right) \end{bmatrix} \quad (4)$$

Besides, the equation of the PMSM's torque is given by (5).

$$T = P_n k_e i_q + P_n\left(L_d - L_q\right) i_d i_q \quad (5)$$

where P_n is number of pole pairs, k_e is the back EMF constant L_d is the d-axis inductance and L_q is the q-axis inductance. When the d-axis current is controlled to zero, the torque of PMSM is proportional to the q-axis current. Then, from (4) and (5), it is confirmed that torque contains the ripples of fundamental frequency components caused by the offset error

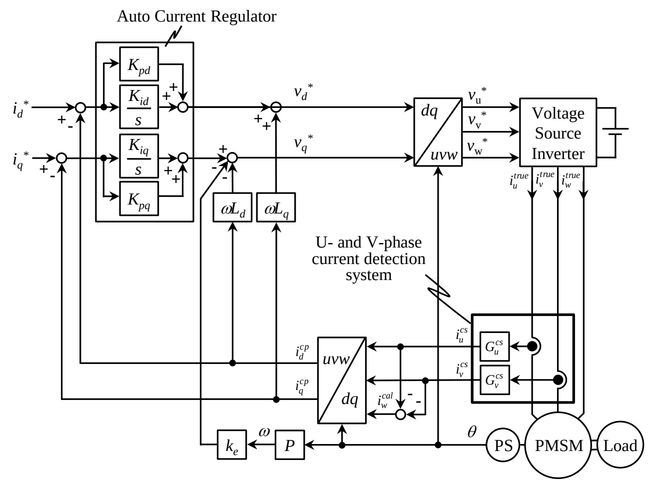

Fig.1. The conventional adjustable speed drive system of IPMSM with two-phase current detection.

of the current sensors and the ripples of the second harmonic components caused by the gain error of the current sensors. Therefore, the correction for gain errors of the current sensors is effective to reduce the torque ripples.

B. Relationship between the current sensor detection errors and the dq-axis voltage commands

When the detected dq-axis currents expressed as (4) are regulated so as to match the dq-axis current commands i_d^* and i_q^* expressed as (6) by conventional PI controller, dq-axis voltage commands v_d^* and v_q^* can be expressed as (7).

$$\begin{bmatrix} i_d^* \\ i_q^* \end{bmatrix} = \frac{I_m^{true}}{\sqrt{3}}\begin{bmatrix} \sin\left(\frac{2}{3}\pi+\phi\right) + \sin\left(\frac{2}{3}\pi-\phi\right) \\ -\cos\left(\frac{2}{3}\pi+\phi\right) + \cos\left(\frac{2}{3}\pi-\phi\right) \end{bmatrix} \quad (6)$$

$$\begin{bmatrix} v_d^* \\ v_q^* \end{bmatrix} = \begin{bmatrix} v_{dini}^* \\ v_{qini}^* \end{bmatrix} + \begin{bmatrix} \left(K_{pd}+\frac{K_{id}}{s}\right)\left(i_d^*-i_d^{cs}\right) \\ \left(K_{pq}+\frac{K_{iq}}{s}\right)\left(i_q^*-i_q^{cs}\right) \end{bmatrix}$$
$$\approx \begin{bmatrix} v_{dini}^* \\ v_{qini}^* \end{bmatrix} + \frac{I_m^{true}}{\sqrt{3}}\begin{bmatrix} \left(K_{pd}+\frac{K_{id}}{s}\right)\left\{\left(1-G_u^{cs}\right)\sin\left(\frac{2}{3}\pi+\phi\right)+\left(1-G_v^{cs}\right)\sin\left(\frac{2}{3}\pi-\phi\right)\right\} \\ \left(K_{pq}+\frac{K_{iq}}{s}\right)\left\{-\left(1-G_u^{cs}\right)\cos\left(\frac{2}{3}\pi+\phi\right)+\left(1-G_v^{cs}\right)\cos\left(\frac{2}{3}\pi-\phi\right)\right\} \end{bmatrix}$$
$$+\frac{2}{\sqrt{3}}\begin{bmatrix} \left(K_{pd}+\frac{K_{id}}{s}\right)\left\{I_{uoffset}^{cs}\sin\left(\theta-\frac{2}{3}\pi\right)-I_{voffset}^{cs}\sin\theta\right\} \\ \left(K_{pq}+\frac{K_{iq}}{s}\right)\left\{I_{uoffset}^{cs}\cos\left(\theta-\frac{2}{3}\pi\right)-I_{voffset}^{cs}\cos\theta\right\} \end{bmatrix}$$
$$+\frac{I_m^{true}}{\sqrt{3}}\begin{bmatrix} \left(K_{pd}+\frac{K_{id}}{s}\right)\left(G_u^{cs}-G_v^{cs}\right)\sin\left(2\theta-\frac{2}{3}\pi+\phi\right) \\ \left(K_{pq}+\frac{K_{iq}}{s}\right)\left(G_u^{cs}-G_v^{cs}\right)\cos\left(2\theta-\frac{2}{3}\pi+\phi\right) \end{bmatrix} \quad (7)$$

where v^*_{dini} is an initial value of the d-axis voltage command, v^*_{qini} is an initial value of the q-axis voltage command, K_{pd} is a d-axis proportion gain, K_{id} is a d-axis integral gain, K_{pq} is a q-axis proportion gain, K_{iq} is a d-axis integral gain and s is the Laplace operator.

3rd term of right hand side of (7) is the fundamental frequency components caused by the current sensor offset error. 4th term of right hand side of (7) is the second components caused by the current sensor gain error.

C. Correction algorithms for the gain unbalance of the current sensor

Fig. 2 shows the two-phase current detection system for driving IPMSM and the control block diagram of the proposed method for the gain unbalance correction. This is a general control system of IPMSM where the proposed correction method for the gain unbalances of the current sensors added. Current sensors are installed in U-phase and V-phase.

In the proposed method, by using the second harmonic components included in the q-axis voltage command value, expressed as 4th term of right hand side of (7), the gain unbalance of the current sensors are corrected. In particular, at first, it extracts the second harmonic components from the q-axis voltage command by using DFT. The DFT is expressed as follows.

$$A_{qk} = \sum_{n=0}^{N-1} a_q(n) e^{-j\frac{2\pi kn}{N}} \tag{8}$$

where N is a number of sampling in one cycle of electrical angle of the motor, k is a harmonic order and $a_q(n)$ is a sampled value.

N is expressed by (9). By substituting k = 2 and (9) to (8), (10) can be calculated. And from this (10), second harmonic components can be extracted from the q-axis voltage command value.

$$N = \frac{2\pi}{\Delta\theta} \tag{9}$$

$$A_{q2} = \sum_{n=0}^{\left(\frac{2\pi}{\Delta\theta}\right)-1} a_q(n) e^{-j2n\Delta\theta} \tag{10}$$

Here, $\Delta\theta$ is determined as follows.

$$\Delta\theta = \frac{2\pi}{4k+m} \quad (m = 0,1,2,\ldots) \tag{11}$$

Then, (12) is obtained by expanding (10) by using an Euler's formula.

$$\begin{aligned} A_{q2} &= \sum_{n=0}^{\left(\frac{2\pi}{\Delta\theta}\right)-1} a_q(n)\{\cos(2n\Delta\theta) - j\sin(2n\Delta\theta)\} \\ &= \sum_{n=0}^{\left(\frac{2\pi}{\Delta\theta}\right)-1} a_q(n)\cdot\cos(2n\Delta\theta) + j\sum_{n=0}^{\left(\frac{2\pi}{\Delta\theta}\right)-1} -a_q(n)\cdot\sin(2n\Delta\theta) \end{aligned} \tag{12}$$

Finally, the second harmonic component v_{q2h}^{ext} included in the d-axis voltage command v^*_q can be extracted by substituting (12) to (13).

$$\begin{aligned} v_{q2h}^{ext} &= \frac{2}{N}\sqrt{(A_{q2})^2}\cos\theta_{q2} \\ &= \frac{\Delta\theta}{\pi}\sqrt{\left\{\sum_{n=0}^{\left(\frac{2\pi}{\Delta\theta}\right)-1} a_q(n)\cos(2n\Delta\theta)\right\}^2 + \left\{\sum_{n=0}^{\left(\frac{2\pi}{\Delta\theta}\right)-1} -a_q(n)\sin(2n\Delta\theta)\right\}^2} \\ &\quad * \cos\left[\tan^{-1}\left\{\frac{\sum_{n=0}^{\left(\frac{2\pi}{\Delta\theta}\right)-1} -a_q(n)\sin(2n\Delta\theta)}{\sum_{n=0}^{\left(\frac{2\pi}{\Delta\theta}\right)-1} a_q(n)\cos(2n\Delta\theta)}\right\}\right] \end{aligned} \tag{13}$$

The extracted second harmonic components v_{q2h}^{ext} from the q-axis voltage command v^*_q is equal to 4th term of right hand side of (7). Therefore, (14) is obtained.

$$v_{q2h}^{ext} = \frac{1}{\sqrt{3}} I_m^{true}\left(K_{pq} + \frac{K_{iq}}{s}\right)\left(G_u^{cs} - G_v^{cs}\right)\cos\left(2\theta - \frac{2}{3}\pi + \phi\right) \tag{14}$$

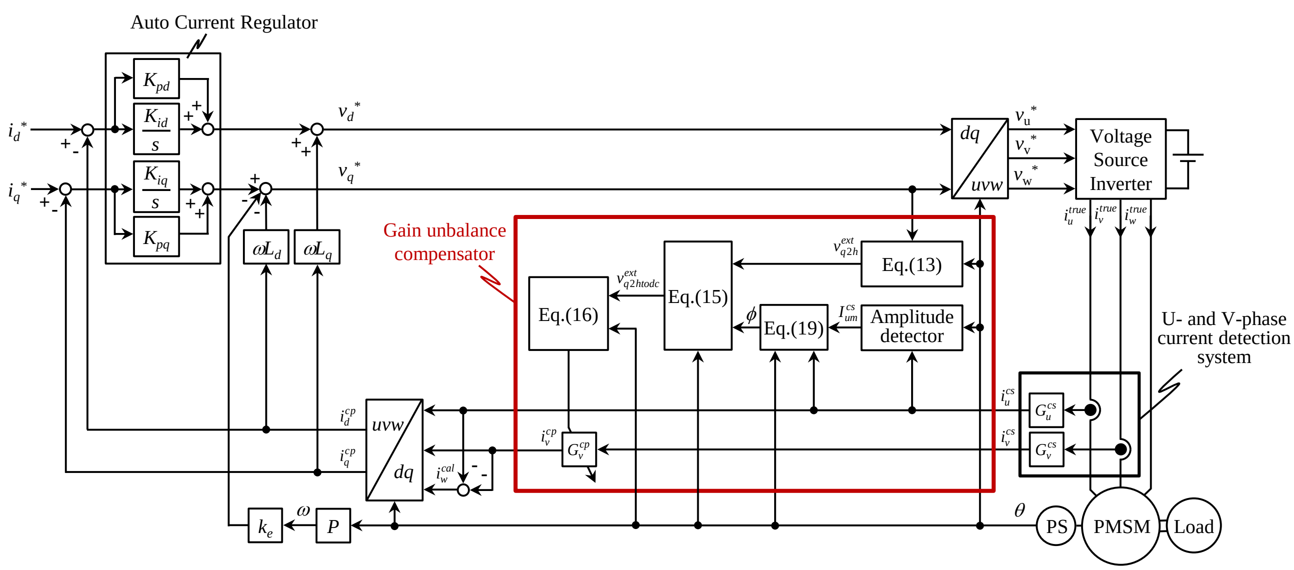

Fig.2. The control block diagram of the proposed method.

By dividing both sides of (14) by $\cos\left(2\theta-\frac{2}{3}\pi+\phi\right)$, (15) is obtained.

$$\frac{v_{q2h}^{ext}}{\cos\left(2\theta-\frac{2}{3}\pi+\phi\right)}=\frac{1}{\sqrt{3}}I_m^{true}\left(K_{pq}+\frac{K_{iq}}{s}\right)\left(G_u^{cs}-G_v^{cs}\right)=v_{q2htodc}^{ext} \quad (15)$$

From (15), it is found that when $v_{q2htodc}^{ext}$ is positive, G_u^{cs} is larger than G_v^{cs}. And when $v_{q2htodc}^{ext}$ is negative, G_u^{cs} is smaller than G_v^{cs}. Based on these relationships, the correction gain of V-phase sensor is increased when $v_{q2htodc}^{ext}$ is positive and the correction gain of V-phase sensor is decreased when $v_{q2htodc}^{ext}$ is negative, as shown in (16).

$$G_v^{cp}=G_{vold}^{cp}+K_{ig}\cdot v_{q2htodc}^{ext} \quad (16)$$

where G_v^{cp} is a correction gain of V-phase sensor, G_{vold}^{cp} is a previous value of correction gain of V-phase sensor and K_{ig} is an integral gain for gain error correction.

The detection gain of V-phase can be matched that of U-phase by multiplying the detection gain of V-phase sensor by the correction gain of V-phase sensor as shown in (17).

$$G_v^{cp}G_v^{cs}=G_u^{cs} \quad (17)$$

Also, the detected current i_u^{cp} from U-phase current sensor can be expressed as (18) by applying the current sensor offset error compensation method in advance. Then, the phase difference ϕ can be calculated by (19).

$$\begin{aligned} i_u^{cs} &\approx G_u^{cs}I_m^{true}\cos(\theta+\phi)+I_{uoffset}^{cs}-\hat{I}_{uoffset}^{cs} \\ &\approx G_u^{cs}I_m^{true}\cos(\theta+\phi) \\ &\approx I_{um}^{true}\cos(\theta+\phi) \end{aligned} \quad (18)$$

$$\phi\approx\cos^{-1}\left(\frac{i_u^{cs}}{I_{um}^{cs}}\right)-\theta \quad (19)$$

where I_{um}^{cs} is the amplitude of the fundamental current detected in U-phase current sensor and $\hat{I}_{uoffset}^{cs}$ is the estimated offset current value of U-phase current sensor.

III. Experimental Results and Simulation Results

Table I shows the experimental conditions. The experimental system for the two–phase-current detection consisted of dc-link voltage of 282 V, a general three-phase VSI, an IPMSM with rated power of 5.5 kW. This section indicates the effectiveness of the proposed method for reducing torque ripple of the second harmonic components caused by the gain unbalance of the current sensors.

Fig.3 shows the experimental waveforms of the q-axis voltage command v_q^* and the extracted second harmonic components v_{q2h}^{ext}, expressed as (13), from v_q^*. The extracted second harmonic components v_{q2h}^{ext} is used for the gain unbalance correction as (15). Also, this components decrease if the gain unbalance of the current sensors is corrected. As a result, the amplitude of v_{q2h}^{ext} is reduced by applying the proposed method.

Table I. Experimental parameters for two-phase-current detection system.

Symbol	Meaning	Value
P_n	Number of pole pairs	3
k_e	Back EMF constant	0.284 [Vs/rad]
L_d	d-axis inductance (typical)	4.3 [mH]
L_q	q-axis inductance (typical)	10.2 [mH]
i_{uoerr}	U-phase current sensor offset error	0 [A]
I_{voerr}	V- phase current sensor offset error	0 [A]
G_u^{cs}	U-phase current sensor gain	1.2
G_v^{cs}	V-phase current sensor gain	0.9
K_{ig}	Integral gain for gain error correction	0.001
$\Delta\theta$	Predetermined amount of motor electric angle change	$\pi/8$

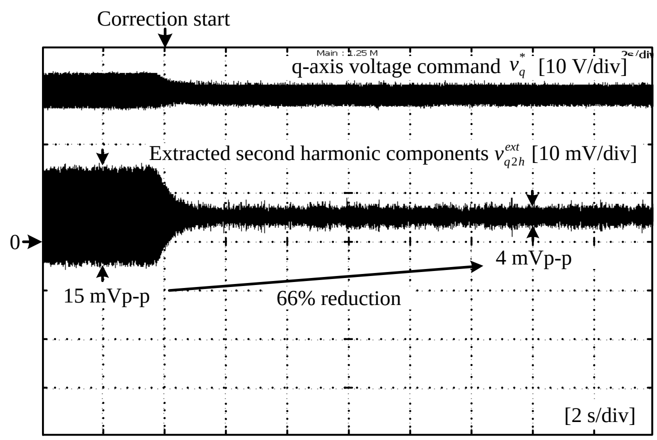

Fig.3. Experimental waveforms of q-axis voltage command and the extracted second harmonic components from q-axis voltage command.

Fig.4 shows the experimental waveforms of gain of U-phase current sensor, the corrected gain of V-phase current sensor expressed as (17) and the calculated torque when the proposed method is applied. Here, it is assumed that the gain errors of the current sensors are within 20% in order to confirm the effectiveness of the proposed method. U-phase and V-phase gain errors of the current sensors set to 1.2 and 0.9, respectively. V-phase gain is corrected with 25% relative error so as to match U-phase gain by applying the proposed method. Also, it is confirmed that the torque ripple is reduced by approximately 50 % by correcting V-phase gain. The gain correction error is caused by low resolution of DFT.

Fig.5 shows the expanded experimental waveforms of the calculated torque. (a) is the waveforms of the calculated torque without the proposed method and (b) is that with the proposed method. Torque ripple of the second harmonic components caused by the gain unbalance of the current sensors is drastically reduced by applying the proposed method.

Fig.6 shows the harmonic analysis results of the torque. It is confirmed that the ripple of second harmonic components caused by the gain unbalance of the current sensors is reduced by 94% by applying the proposed method. Here, remaining torque ripples of 6^{th}-order components and 12^{th}-order components are resulting from the spatial harmonics of permanent magnet flux and the dead time of inverter.

IV. Conclusion

This paper presents a new algorithm which can correct the gain unbalance of the current sensors in the conventional two-phase current detection system for driving IPMSM by using the second harmonic components included in the q-axis voltage command value. From experimental results, it is confirmed that the torque ripple is reduced by 50% by correcting the gain unbalance of the current sensors, in particular, by matching V-phase gain and U-phase gain. From harmonic analysis results, the torque ripple of second harmonic components caused by the gain unbalance of current sensors is reduced by 94%.

References

[1] M. Gaiceanu and A. Minzararu: "Optimal control of permanent magnet synchronous machines for cold rolling mills", ISEEE 2010, pp. 105-111, 2010.

[2] K. Kondo and M. Kondo: "Design of the parameters of permanent magnet synchronous motors for railway vehicle traction", PEDS 2003, Vol. 2, pp. 992-997, 2003.

[3] G. Maggetto and J. Van Mierlo: "Electric and electric hybrid vehicle technology: a survey", IEE Seminar Electric, Hybrid and Fuel Cell Vehicles", pp.1-11, 2000.

[4] Han-Su Jung, Seon-Hwan Hwang, Jang-Mok Kim, Cheul-U Kim and Cheol Choi: "Diminution of current-measurement error for vector-controlled AC motor drives", IEEE Trans. on IA, Vol. 42, No. 5, pp. 1249-1256, 2006.

[5] Kyung-Rae Cho and Jul-Ki Seok: "Correction on current-measurement errors for accurate flux estimation of AC drives at low stator frequency", IEEE Trans. on IA, Vol. 44, No. 2, pp.594-603, 2008.

[6] Myoungho Kim, Seung-Ki Sul and Junggi Lee: "Compensation of current measurement error for current controlled-PMSM drives", IEEE Trans. on IA, Vol. 50, No. 5, pp. 3365-3373, 2014.

[7] H. Tamura, T. Ajima and Y. Noto: "A torque ripple reduction method by current sensor offset error compensation", EPE 2013, pp. 1-10, 2013.

[8] H. Tamura, T. Ajima, Y. Noto and J. Itoh: "A compensation method for a motor phase current sensor offset error using a voltage-source-inverter output voltage reference value", EPE 2014, pp.1-10, 2014.

[9] H. Tamura, T. Ajima, Y. Noto and J. Itoh: "A Novel Compensation Method for a Motor Phase Current Sensor Offset Error Varied during a VSI-Motor Drive", IPEC 2014, pp. 682-688, 2014.

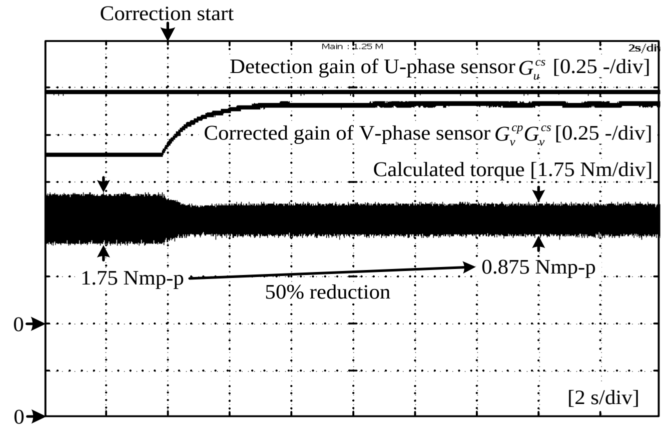

Fig.4. Experimental waveforms of the gains of U and V-phase current sensors and the calculated torque when the proposed method is applied.

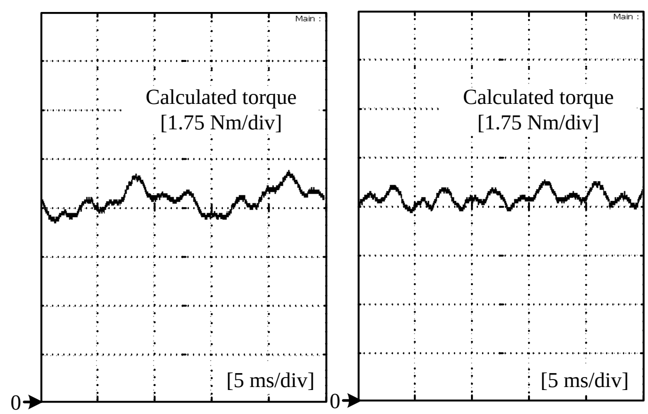

(a) Without the proposed method. (b) With the proposed method.

Fig.5. Expanded experimental waveforms of the calculated torque.

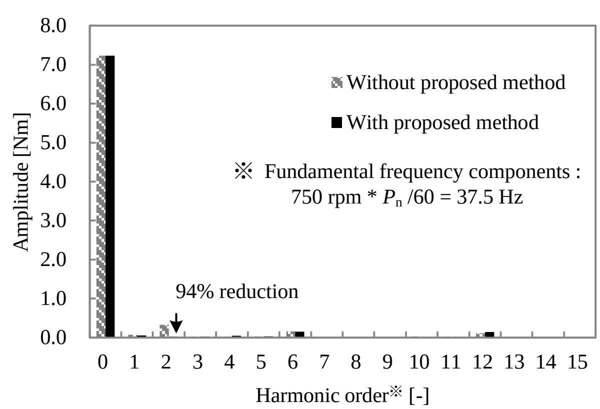

Fig.6. Harmonic analysis results of torque ripples.